

Identification of muscle forces in human lower limbs during sagittal plane movements Part I: Human body modelling

WOJCIECH BLAJER, KRZYSZTOF DZIEWIECKI, ZENON MAZUR

Institute of Applied Mechanics, Technical University of Radom

The paper presents a human biomechanical model aimed at determining muscle forces during planar movements such as standing long jumps, vertical jumps and jumps down from a height. Only the hip, knee and ankle joints are modelled as directly enforced by the muscle forces applied to their tendon attachment points, and the actuation of the other joints is simplified to torques representing the muscle action. A systematic construction of the related dynamic equations in independent coordinates is provided, followed by some guidelines for their use in analysing motion during the flying and support phases.

1. Introduction

The understanding of how human beings are maneuvered can be interesting from many viewpoints. The determination of muscle forces during movement contributes to the elucidation of the underlying neural control and is essential for a complex analysis of internal loads acting on bones and joints; both of considerable importance to clinicians [1]. The ways the humans are moved/controlled are then also widely imitated in engineering designs like robots, manipulators and walking machines. Since the measuring of muscle forces directly within the living beings may be difficult and even injurious, the other possibility is to estimate them computationally based on a biomechanical model and some input data obtained from noninvasive measurements. The need for reliable results obtained this way has stimulated an increased interest in thorough human body modelling and advanced computational algorithms [2], [3]. This paper is another contribution in this field.

The inherent complexity of human body always calls for some modelling simplifications, and the mathematical models should in general be as complex as necessary and as simple as possible, which is always a compromise between the analysis thoroughness and modelling feasibilities. The biomechanical model developed in this paper is aimed at

analyzing human movements such as standing long jumps, vertical jumps and jumps down from a height, in which the lower and upper extremities are moving parallel to each other in the sagittal plane. For these reasons we decided for a planar model of human body, in which the modelled muscle forces are in fact their projections onto the sagittal plane. Then, since the attention is focused on lower limb control and loadings, only the hip, knee and ankle joints are modelled as enforced directly by the muscle forces applied to their tendon attachment points, and the actuation of the other joints is simplified to torques representing the muscle action. In this first part of the paper, we present the foundations for the design of the biomechanical model. A systematic construction of the related dynamic equations in independent coordinates is then provided, followed by some guidelines for their use in the analysis of motion during the flying and support phases.

2. Modelling preliminaries

The human body is modelled as a planar kinematic structure consisting of $N = 9$ rigid bodies branching from the pelvis in the open chain linkages (see figure 1). The $n = 11$ generalized coordinates that describe the position of the ‘flying’ model with respect to the inertial reference frame are $\mathbf{q} = [x_H \ y_H \ \varphi_1 \ \dots \ \varphi_9]^T$, where x_H and y_H are the coordinates of the hip point H , and the angular coordinates φ_i ($i=1, \dots, N$) are all measured from the vertical direction. The n -degree-of-freedom system is actuated by $k = 8$ torques $\mathbf{u}' = [\tau_1 \ \dots \ \tau_8]^T$ representing the muscle action in the joints – the system is thus underactuated in the flying phase, $k < n$.

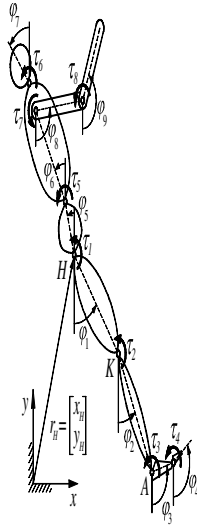


Fig. 1. The human biomechanical model



Fig. 2. The muscles in lower limbs

The attention of this study is focused on the lower limb control and loadings during sagittal movements. The actuation in the hip, knee and ankle joints needs thus a more detailed modelling. We identified $m_F = 15$ muscles that produce the control torques in the three joints (see figure 2), and the respective muscle forces F_1, \dots, F_{15} applied to their tendon attachment points are treated as control inputs instead of τ_1 , τ_2 and τ_3 . The total vector of $m = m_F + m_\tau = 20$ control inputs is then $\mathbf{u} = [F_1 \dots F_{15} \tau_4 \dots \tau_8]^T$, where $m_\tau = 5$ are the control torques in the other joints (note that τ_5^* included in \mathbf{u} is slightly different from τ_5 represented in \mathbf{u}'). Since the m_F muscle forces actuate the motion in the three joints H , K and A , a local control redundancy is faced, which will be discussed in more detail in part II of this paper.

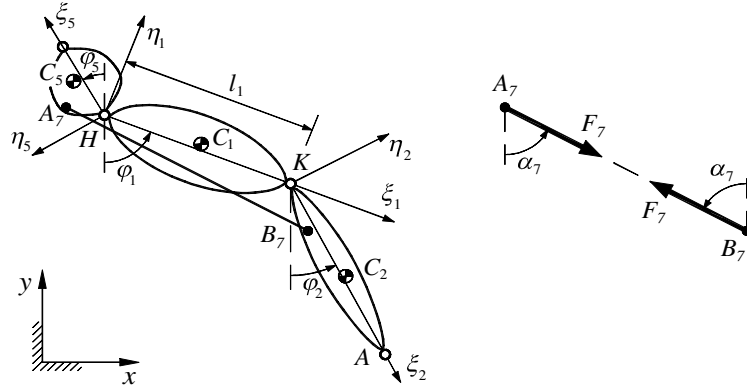


Fig. 3. The tendon attachment points of the 7-th muscle

Using $3N = 27$ absolute coordinates $\mathbf{p} = [x_{C1} \ y_{C1} \ \theta_1 \ \dots \ x_{C9} \ y_{C9} \ \theta_9]^T$, where x_{C_i} , y_{C_i} and θ_i are the coordinates of the mass center C_i and the orientation angle (here $\theta_i = \varphi_i$) of the i -th body segment with respect to the inertial frame, $i = 1, \dots, N$, the dynamic equations of the flying model expressed in \mathbf{p} are the constrained Newton–Euler equations in the form

$$\mathbf{M}\ddot{\mathbf{p}} = \mathbf{f}_g + \mathbf{B}\mathbf{u} - \mathbf{C}^T\boldsymbol{\lambda}, \quad (1)$$

where $\mathbf{M} = \text{diag}(m_1, m_1, J_{C1}, \dots, m_9, m_9, J_{C9})$ is the generalized mass matrix related to \mathbf{p} , m_i and J_{C_i} are the mass and mass moment of inertia with respect to C_i of the i -th segment, $\mathbf{f}_g = [0 \ -m_1g \ 0 \ \dots \ 0 \ -m_9g \ 0]^T$ contains the gravitational forces, $\mathbf{f}_u = \mathbf{B}\mathbf{u}$

is the $3N$ -vector of generalized control forces, with \mathbf{B} being the $3N \times m$ matrix of distribution of control inputs \mathbf{u} in the directions of \mathbf{p} , and $\mathbf{f}_c = -\mathbf{C}^T \boldsymbol{\lambda}$ is the $3N$ -vector of generalized reaction forces due to the $l = 2k = 16$ kinematical joint constraints, with \mathbf{C} being the $l \times 3N$ constraint matrix and $\boldsymbol{\lambda} = [\lambda_1 \dots \lambda_l]^T$ containing the reaction forces in the joints.

The formulation of \mathbf{M} and \mathbf{f}_g in equation (1) is evident, and the same concerns the last m_τ columns of \mathbf{B} related to τ_4, \dots, τ_8 – their entries are either 0, 1 or -1 (see [4] for more details). For example, the 19-th column of \mathbf{B} , related to τ_7 , has all the entries equal to zero except the 24-th and 18-th entries (related to θ_8 and θ_6), which are equal to 1 and -1 , respectively. The determination of the first m_F columns of \mathbf{B} , related to F_1, \dots, F_{15} , is a little more challenging. Let us demonstrate this for the case of the 7-th column of \mathbf{B} , related to F_7 (figure 2). Firstly, we must state that the 7-th muscle tendons are attached to segments 2 and 5, and only these two bodies are directly affected by F_7 . This also means that only those entries of the 7-th column of \mathbf{B} that correspond to these two bodies must be found, and the other entries are in principle equal to zero. The indices of nonzero entries are from 4 to 6 (body 2) and from 13 to 15 (body 5). The second step is determination of the inertial frame coordinates $\mathbf{r}_{A7} = [x_{A7} \ y_{A7}]^T$ and $\mathbf{r}_{B7} = [x_{B7} \ y_{B7}]^T$ of tendons attachment points A_7 and B_7 (see figure 3), which are:

$$\begin{aligned} x_{A7} &= x_H - \xi_{A7} \cos \theta_5 - \eta_{A7} \sin \theta_5, \\ y_{A7} &= y_H + \xi_{A7} \sin \theta_5 - \eta_{A7} \cos \theta_5, \\ x_{B7} &= x_H + l_1 \sin \theta_1 + \xi_{B7} \sin \theta_2 + \eta_{B7} \cos \theta_2, \\ y_{B7} &= y_H - l_1 \cos \theta_1 - \xi_{B7} \cos \theta_2 + \eta_{B7} \sin \theta_2, \end{aligned} \quad (2)$$

where $\boldsymbol{\rho}_{A7} = [\xi_{A7} \ \eta_{A7}]^T$ and $\boldsymbol{\rho}_{B7} = [\xi_{B7} \ \eta_{B7}]^T$ are the coordinates of A_7 and B_7 in the local coordinate systems of segments 5 and 2, respectively, and l_1 is the length of segment 2. The nonzero entries of the 7-th column of \mathbf{B} are then:

$$\begin{aligned} B_{4,7} &= -\sin \alpha_7, \\ B_{5,7} &= \cos \alpha_7, \\ B_{6,7} &= (y_{B7} - y_{C2}) \sin \alpha_7 - (x_{C2} - x_{B7}) \cos \alpha_7, \\ B_{13,7} &= \sin \alpha_7, \\ B_{14,7} &= -\cos \alpha_7, \\ B_{15,7} &= (y_{C5} - y_{A7}) \sin \alpha_7 + (x_{C5} - x_{A7}) \cos \alpha_7, \end{aligned} \quad (3)$$

where $\mathbf{r}_{C5} = [x_{C5} \ y_{C5}]^T$ and $\mathbf{r}_{C2} = [x_{C2} \ y_{C2}]^T$ of mass centers C_5 and C_2 can be determined from equation (2) using $\mathbf{p}_{C5} = [\xi_{C5} \ \eta_{C5}]^T$ and $\mathbf{p}_{C2} = [\xi_{C2} \ \eta_{C2}]^T$ instead of \mathbf{p}_{A7} and \mathbf{p}_{B7} , and

$$\sin \alpha_7 = \frac{x_{B7} - x_{A7}}{\sqrt{(x_{B7} - x_{A7})^2 + (y_{A7} - y_{B7})^2}}, \quad \cos \alpha_7 = \frac{y_{A7} - y_{B7}}{\sqrt{(x_{B7} - x_{A7})^2 + (y_{A7} - y_{B7})^2}}. \quad (4)$$

Following the above procedure for all forces F_j , $j = 1, \dots, m_F$, the first m_F columns of \mathbf{B} can be determined. Then, augmenting them by the last m_τ columns of \mathbf{B} defined above, the whole $3N \times m$ matrix \mathbf{B} can be formulated.

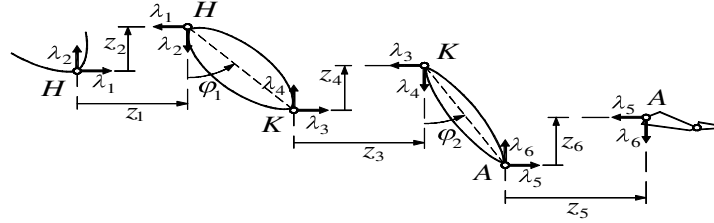


Fig. 4. The open-constraint coordinates and the reaction forces in lower extremity joints

The $l \times 3N$ constraint matrix \mathbf{C} in equation (1) follows from the joint constraint equations

$$\Phi(\mathbf{p}) = \mathbf{0} \quad \Rightarrow \quad \dot{\Phi} = \mathbf{C}(\mathbf{p})\dot{\mathbf{p}} = \mathbf{0}, \quad (5),(6)$$

i.e., $\mathbf{C} = \partial\Phi/\partial\mathbf{p}$. Since all the k joints in the system are rotary, at each joint two constraint equations expressing the prohibited relative x and y translations are introduced, denoted open-constraint coordinates $\mathbf{z} = [z_1 \ \dots \ z_l]^T$, where $l = 2k$ [4]. The constraint equations are then $\mathbf{z} = \Phi(\mathbf{p}) = \mathbf{0}$, and a particular constraint equation $\Phi_i(\mathbf{p}) = 0$ ($i = 1, \dots, l$) depends only on the absolute coordinates of the adjacent bodies in the respective joint. The open-constraint coordinates in the lower extremity joints H , K and A and the related reaction forces are illustrated in figure 4. As an example, the two constraint equations related to K joint are:

$$\begin{aligned} \Phi_3 &= x_{C2} - \xi_{C2} \sin \theta_2 - \eta_{C2} \cos \theta_2 - [x_{C1} + (l_1 - \xi_{C1}) \sin \theta_1 - \eta_{C1} \cos \theta_1] = 0, \\ \Phi_4 &= y_{C2} + \xi_{C2} \cos \theta_2 - \eta_{C2} \sin \theta_2 - [y_{C1} - (l_1 - \xi_{C1}) \cos \theta_1 + \eta_{C1} \sin \theta_1] = 0. \end{aligned} \quad (7)$$

The third and fourth rows of \mathbf{C} can then be constructed, not reported here for shortness, whose nonzero entries will relate only the absolute coordinates of segments 1 and 2.

3. Dynamic equations in independent coordinates

The projective formulation of *joint coordinate method* described in [5] is applied to derive the dynamic equations of the human biomechanical model in coordinates \mathbf{q} . The scheme is based on the relationships between the absolute (dependent) coordinates \mathbf{p} and the independent coordinates \mathbf{q} , which state the joint constraint equations given explicitly. At the position, velocity and acceleration levels the explicit constraint equations are:

$$\mathbf{p} = \mathbf{g}(\mathbf{q}) \Rightarrow \dot{\mathbf{p}} = \mathbf{D}(\mathbf{q})\dot{\mathbf{q}} \Rightarrow \ddot{\mathbf{p}} = \mathbf{D}(\mathbf{q})\ddot{\mathbf{q}} + \boldsymbol{\gamma}(\mathbf{q}, \dot{\mathbf{q}}), \quad (8),(9),(10)$$

where $\mathbf{D} = \partial \mathbf{g} / \partial \mathbf{q}$ is the $3N \times n$ matrix, and $\boldsymbol{\gamma} = \dot{\mathbf{D}}\dot{\mathbf{q}}$ is the $3N$ vector. As an example, the absolute coordinates of segment 3 can be expressed in \mathbf{q} as follows:

$$\begin{aligned} x_{C3} &= x_H + l_1 \sin \varphi_1 + l_2 \sin \varphi_2 + \xi_{C3} \sin \varphi_3 + \eta_{C3} \cos \varphi_3, \\ y_{C3} &= y_H - l_1 \cos \varphi_1 - l_2 \cos \varphi_2 - \xi_{C3} \cos \varphi_3 + \eta_{C3} \sin \varphi_3, \\ \theta_3 &= \varphi_3, \end{aligned} \quad (11)$$

which make the seventh, eighth and ninth entries of equation (8). After introducing the other components of $\mathbf{p} = \mathbf{g}(\mathbf{q})$, \mathbf{D} and $\boldsymbol{\gamma}$ defined in equations (9) and (10) can be obtained.

Since $\boldsymbol{\Phi}(\mathbf{g}(\mathbf{q})) \equiv \mathbf{0}$, after inserting equations (8) and (9) into equation (6), it can be deduced that $\mathbf{C}(\mathbf{g}(\mathbf{q}))\mathbf{D}(\mathbf{q})\dot{\mathbf{q}} \equiv \mathbf{0}$, and thus $\mathbf{C}\mathbf{D} = \mathbf{0} \Leftrightarrow \mathbf{D}^T\mathbf{C}^T = \mathbf{0}$ – the $3N \times n$ matrix \mathbf{D} is an orthogonal complement to the $l \times 3N$ constraint matrix \mathbf{C} in the $3N$ -dimensional configuration space related to \mathbf{p} [5]. The dynamic equations (1), defined in the $3N$ -dimensional linear space related to $\dot{\mathbf{p}}$, can then be projected into the n -dimensional tangential (velocity allowed) and l -dimensional constrained (null velocity) subspaces, defined by the vectors represented as columns of \mathbf{D} and rows of \mathbf{C} . The projection formula is (see [5] for more details)

$$\begin{bmatrix} \mathbf{D}^T \\ \mathbf{C}\mathbf{M}^{-1} \end{bmatrix} (\mathbf{M}(\mathbf{D}\ddot{\mathbf{q}} + \boldsymbol{\gamma}) - \mathbf{f}_g - \mathbf{B}\mathbf{u} + \mathbf{C}^T\boldsymbol{\lambda}) = \mathbf{0}, \quad (12)$$

where equation (10) was substituted for $\ddot{\mathbf{p}}$. Considering that $\mathbf{D}^T\mathbf{C}^T = \mathbf{0}$, the first n equations lead to the requested dynamic equations in \mathbf{q} , whose matrix generic form is

$$\overline{\mathbf{M}}\ddot{\mathbf{q}} + \overline{\mathbf{d}} = \overline{\mathbf{f}}_g + \overline{\mathbf{B}}\mathbf{u}, \quad (13)$$

where $\overline{\mathbf{M}}(\mathbf{q}) = \mathbf{D}^T \mathbf{M} \mathbf{D}$ is the $n \times n$ generalized mass matrix related to \mathbf{q} ; $\overline{\mathbf{d}}(\mathbf{q}, \dot{\mathbf{q}}) = \mathbf{D}^T \mathbf{M} \boldsymbol{\gamma}$ and $\overline{\mathbf{f}}_g = \mathbf{D}^T \mathbf{f}_g$ are the n -vectors of generalized dynamic forces related to \mathbf{q} due to the centrifugal accelerations and gravitational forces, respectively, and $\overline{\mathbf{B}} = \mathbf{D}^T \mathbf{B}$ is the $n \times m$ matrix of the distribution of the control inputs \mathbf{u} in the directions of \mathbf{q} .

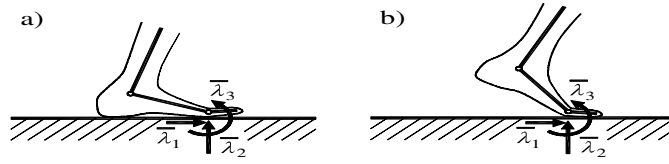


Fig. 5. The foot in contact with the ground

The dynamic equation (13) describes the human body dynamics in the flying phase. During the support phase, when the feet are in contact with the ground, $r = 3$ additional constraints are imposed on the system, written symbolically as $\overline{\Phi}(\mathbf{q}) = \mathbf{0}$. For the two contact modes seen in figure 5, these constraint equations are:

$$\begin{aligned} \overline{\Phi}_1 &= x_H + l_1 \sin \varphi_1 + l_2 \sin \varphi_2 + l_3 \sin \varphi_3 - x_0 = 0, \\ \overline{\Phi}_2 &= y_H - l_1 \cos \varphi_1 - l_2 \cos \varphi_2 + l_3 \cos \varphi_3 - y_0 = 0, \\ \overline{\Phi}_3^{(a)} &= \varphi_3 - \pi/2 = 0 \quad \text{or} \quad \overline{\Phi}_3^{(b)} = \varphi_4 - \pi/2 = 0, \end{aligned} \quad (4)$$

where x_0 and y_0 are the inertial frame coordinates of the point to which the reactions from the ground $\bar{\lambda} = [\bar{\lambda}_1 \ \bar{\lambda}_2 \ \bar{\lambda}_3]^T$ are reduced. For both modes of the foot-ground contact seen in figure 5 we reduce the ground reaction to the same point – the end of instep (segment 3).

The ground-contact constraint equations at the velocity and acceleration levels are $\overline{\mathbf{C}}\dot{\mathbf{q}} = \mathbf{0}$ and $\overline{\mathbf{C}}\ddot{\mathbf{q}} - \overline{\xi} = \mathbf{0}$, respectively, where $\overline{\mathbf{C}}(\mathbf{q}) = \partial \overline{\Phi} / \partial \mathbf{q}$ is the $r \times n$ constraint matrix and $\overline{\xi}(\mathbf{q}, \dot{\mathbf{q}}) = -\dot{\overline{\mathbf{C}}}\dot{\mathbf{q}}$ is the n -vector of constraint-induced accelerations [5]. The dynamic equations (13) modify then to $\overline{\mathbf{M}}\ddot{\mathbf{q}} + \overline{\mathbf{d}} = \overline{\mathbf{f}}_g + \overline{\mathbf{B}}\mathbf{u} - \overline{\mathbf{C}}^T \bar{\lambda}$. Introducing an $n \times k$ ($k = n - r = 8$) matrix $\overline{\mathbf{D}}$ such that $\overline{\mathbf{C}}\overline{\mathbf{D}} = \mathbf{0} \Leftrightarrow \overline{\mathbf{D}}^T \overline{\mathbf{C}}^T = \mathbf{0}$ and using the

projection formula similar to that used in equation (12), the tangential and orthogonal projections give respectively:

$$\overline{\mathbf{D}}^T \overline{\mathbf{M}} \ddot{\mathbf{q}} = \overline{\mathbf{D}}^T (\overline{\mathbf{f}}_g - \overline{\mathbf{d}} + \overline{\mathbf{B}} \mathbf{u}), \quad (15)$$

$$\overline{\boldsymbol{\lambda}}(\mathbf{q}, \dot{\mathbf{q}}, \mathbf{u}) = (\overline{\mathbf{C}} \overline{\mathbf{M}}^{-1} \overline{\mathbf{C}}^T)^{-1} (\overline{\mathbf{C}} \overline{\mathbf{M}}^{-1} (\overline{\mathbf{f}}_g - \overline{\mathbf{d}} + \overline{\mathbf{B}} \mathbf{u}) - \overline{\boldsymbol{\xi}}). \quad (16)$$

Equation (15) constitutes the ground reaction-free dynamic equations of the modeled human during the support phase. Note that the number k of these equations is equal to the number of control torques \mathbf{u}' at the k joints, distributed then in joints H , K and A into m_F muscle forces. Equation (16) supplies one with a formula for determination of the ground reaction values.

4. Conclusions

In this first part of the paper, we presented foundations and systematic construction of a human body biomechanical model aimed at analyzing planar movements such as vertical or standing long jumps. A hybrid model of control was used, modelled by means of muscle forces in the lower extremity joints, and simplified to the torques representing the muscle action at the other joints. Two different sets of motion equations were derived, separately for the flying phase and the support phase. The ground reactions during the support phase can also be determined. In the second part of the paper [6], applications of the developed mathematical model to the inverse dynamics analysis of human movements will be discussed.

References

- [1] WISMANS J.S.H.M., JANSSEN E.G., BEUSENBERG M., KOPPENS W.P., LUPKER H.A., *Injury biomechanics*, Course notes, Faculty of Mechanical University, Eindhoven University of Technology, Eindhoven, 1994.
- [2] TÖZEREN A., *Human body dynamics: classical mechanics and human movement*, Springer, New York, 2000.
- [3] TAMAGUCHI G.T., *Dynamic modeling of musculoskeletal motion*, Kluwer, Norwell, 2001.
- [4] BLAJER W., CZAPLICKI A., *Contact modeling and identification of planar somersaults on the trampoline*, *Multibody System Dynamics*, 2003, 10, 289–312.
- [5] BLAJER W., *Methods of multibody dynamics* (in Polish), Monographs, No. 35, Press of the Technical University of Radom, Radom, 1998.
- [6] BLAJER W., DZIEWIECKI K., MAZUR Z., *Identification of muscle forces in lower limbs during sagittal plane movements. Part II: Computational algorithms* (ibidem).